IOSR Journal Of Applied Physics (IOSR-JAP)
e-ISSN: 2278-4861.Volume 18, Issue 4 Ser. 1 (July – August 2026), PP 24-35
www.Iosrjournals.Org

Valorization Of Sewage Sludge Waste: Performance Of Nano-Scale Sludge Filler In Natural Rubber Composites

D. I. Moubarak
Mechatronics Department, Faculty Of Technological Industry And Energy, Delta Technological University, Qeweisna, 32632, Menofia, Egypt

Corresponding E-mail: dr.dmobark@dtu.edu.eg

Abstract
Sewage sludge management remains an environmental and economic challenge because of the large quantities generated by municipal wastewater treatment plants and the increasing limitations of conventional disposal routes. In this study, dewatered municipal sludge was processed by drying, grinding, and high-energy ball milling to produce a nano-scale sewage sludge (NSS) filler for natural rubber (NR) composites. The filler was incorporated into NR at loadings of 0–50 phr, and the resulting composites were evaluated in terms of morphology, hardness, tensile response, swelling behavior, solvent transport, and thermal characteristics.
Morphological analysis confirmed the heterogeneous fine-particle nature of the processed sludge and showed that filler distribution remained more uniform at intermediate loading, while agglomeration became more evident at higher loading. Relative to unfilled NR, NSS-filled composites exhibited increased hardness and tensile modulus, together with reduced kerosene uptake and lower apparent diffusion behavior, indicating greater resistance to solvent penetration and reduced swelling tendency. Thermal analysis further showed that NSS loading increased the residual fraction after heating and altered the decomposition profile of the composites, mainly because of the inorganic/mineral content of the sludge-derived filler.
Overall, the results demonstrate that sewage sludge can be converted into a functional waste-derived filler for NR composites. The findings show that NSS can improve stiffness, hardness, and swelling resistance, while the final balance of properties remains strongly dependent on filler loading, dispersion state, and agglomeration behavior at higher concentrations.

Keywords: *Natural Rubber (NR), Sewage Sludge Fillers, Mechanical Properties, Composite Materials, Recycled Material*

Date of Submission: 01-08-2026 Date of Acceptance: 11-08-2026

I. Introduction

Sewage sludge is one of the most persistent by-products of municipal wastewater treatment and continues to represent an environmental and economic management challenge because of its large generation volume, variable composition, and increasingly restricted disposal routes. Conventional practices such as land application, landfilling, and incineration are often constrained by regulatory, environmental, and cost considerations [1–4]. As a result, sewage sludge valorization has attracted increasing attention as part of a broader circular-economy strategy aimed at converting waste streams into value-added materials [3, 4].

In parallel, the rubber industry continues to seek lower-cost and more sustainable alternatives to conventional fillers, especially for applications in which partial substitution by waste-derived solids may be feasible. The performance of filled rubber compounds depends strongly on filler loading, particle size, dispersion quality, and filler-rubber interfacial interaction [5, 6]. Related studies on recycled glass-derived fillers in rubber systems have likewise shown that the final mechanical and thermal performance depends strongly on filler loading, dispersion quality, and matrix-filler compatibility, with intermediate filler contents often providing a more favorable balance than excessive loading [7, 8]. Accordingly, waste-derived fillers cannot be evaluated solely on the basis of their origin; rather, they must be assessed in terms of how they modify morphology, deformation behavior, solvent transport, and thermal response within the elastomer matrix [5–7].

Natural rubber (NR) is an attractive matrix for such studies because of its wide industrial use, high elasticity, and strong sensitivity to filler-induced changes in stiffness, fracture behavior, and swelling resistance [5, 9]. For example, recycled micro-glass fillers have previously been reported to modify the stiffness and thermal response of NR composites, while related glass-filled SBR/NBR systems also showed loading-dependent mechanical changes associated with dispersion and aggregation effects [7, 8]. However, the use of sewage-sludge-derived particulate fillers in NR remains insufficiently explored, particularly when the sludge is processed to a fine or nano-scale form intended to improve dispersion and increase interfacial area. This is

important because sludge-derived fillers contain both carbonaceous and inorganic constituents, and these two fractions may influence the rubber compound differently in terms of stiffness development, solvent uptake, and thermal residue formation [9–12].

The present work investigates the use of nano-scale sewage sludge (NSS), prepared from dewatered municipal biosolids through drying, grinding, and high-energy milling, as a waste-derived filler for NR composites. The study focuses on the influence of NSS loading on filler morphology, thermal-response behavior, hardness, tensile response, and kerosene-swelling characteristics. Rather than treating sewage sludge simply as a disposal burden, this work examines its potential as a functional filler in elastomer formulations, while also considering the limitations introduced by filler agglomeration and compositional heterogeneity at higher loading levels.

II. Experimental

Materials

Natural rubber (NR) of technically specified rubber grade TSR-20 was used as the base polymer matrix. The rubber was supplied in bale form and had a Mooney viscosity of approximately ML(1+4) at 100 °C of about 70.

The waste-derived filler used in this study was prepared from dewatered municipal sewage sludge (biosolids) collected from a local wastewater treatment plant. To convert the raw sludge into a stable and processable solid feedstock, the material was first air-dried under a fume hood for 48 h and then oven-dried at 105 °C to constant mass in order to minimize residual moisture. The dried solids were subsequently ground and subjected to high-energy ball milling to produce the nano-scale sewage sludge (NSS) filler used in the rubber compounds.

Zinc oxide (ZnO) and stearic acid were used as vulcanization activators, N-isopropyl- N′-phenyl- p-phenylenediamine (IPPD, 4020) was used as an antioxidant, 2,2′-dibenzothiazyl disulfide (MBTS) was used as the accelerator, and sulfur was used as the vulcanizing agent. A commercially available naphthenic oil was used as the processing oil/plasticizer to facilitate filler incorporation and improve compound processability during milling.

Sample Preparation and Compounding of NR/NSS Composites

NR/NSS compounds were prepared on a laboratory two-roll mill. The natural rubber was first masticated for approximately 5 min until a smooth and uniform rubber band was formed on the front roll. NSS was then introduced gradually at filler loadings of 0, 10, 20, 30, 40, and 50 phr (parts per hundred parts of rubber by weight). The filler was added in small increments along the nip to promote more uniform distribution and to reduce local overloading.

After the initial incorporation of NSS, naphthenic oil (10 phr) was added to assist filler wetting, facilitate dispersion, and improve the processability of the compound during milling. Once the filler–oil–rubber mixture became visually homogeneous, the remaining ingredients were added sequentially: ZnO (5 phr), stearic acid (2 phr), IPPD (1 phr), MBTS (2 phr), and sulfur (2 phr). To minimize premature vulcanization, the curatives were introduced during the final stage of mixing. Throughout compounding, cooling water was circulated to maintain the roll temperature below 70 °C.

After mixing, the compounded sheets were removed from the mill, sheeted to a thickness of approximately 4 mm, and allowed to rest at room temperature for 24 h prior to curing. Vulcanization was then carried out in a hydraulic hot press at 150 °C under a pressure of approximately 14.7 MPa. The cure time was selected on the basis of rheometric determination. Standard test specimens were subsequently die-cut from the cured sheets and conditioned at 23 ± 2 °C before characterization. The compound formulations are summarized in Table 1.

Table 1 Formulation of NR/NSS compounds

Ingredients	Phr*	Function
Natural Rubber (NR)	100	Elastomeric Matrix
Zinc Oxide (ZnO)	5	Activator
Stearic Acid	2	Activator / Processing Aid
Processing Oil (Naphthenic Oil)	10	Plasticizer / Processing aid
IPPD (4020)	1	Antioxidant
MBTS	2	Accelerator
Sulfur	2	Vulcanizing Agent
NSS	0, 10, 20, 30, 40, 50	Sustainable Nano-filler

**Phr: Parts per hundred parts of rubber by weight.*

Characterization Techniques

Tensile properties were measured on a universal testing machine in accordance with ASTM D412. Type-C dumbbell specimens were clamped with acentric wheel grips and stretched at a crosshead speed of 500 mm min ^{1} until rupture. Tensile strength, elongation at break, and moduli were calculated, and each reported value represents the average of at least five specimens from different regions of the sheet.

Shore A hardness was measured according to ASTM D2240 using a calibrated durometer. The reported values correspond to the average of multiple readings on conditioned specimens.

The morphology of the NSS filler and the fracture surfaces of the composites were examined using transmission electron microscopy (TEM) and scanning electron microscopy (SEM). Elemental composition was analyzed by energy-dispersive X-ray spectroscopy (EDX) [13, 14]. The textural properties of the NSS filler were further investigated by nitrogen adsorption/desorption analysis at 77 K. Surface-area and pore-structure characteristics were evaluated using multipoint BET, BJH, and DFT-based analyses [15–17]. In the revised manuscript, the porosity discussion is based primarily on the BJH and DFT outputs, which confirmed the porous nature of the filler and provided pore-size and pore-volume information.

Thermal behavior was evaluated by thermogravimetric analysis (TGA) and derivative thermogravimetry (DTG) under nitrogen atmosphere to examine decomposition behavior and residual mass. Differential scanning calorimetry (DSC) was also used to compare the heat-flow response of the different formulations.

Swelling behavior was investigated through kerosene-immersion tests in order to assess solvent uptake, transport behavior, and swelling-related network restriction in the vulcanized NR/NSS composites. Square specimens of approximately 1 cm × 1 cm × 0.1 cm were cut from the cured sheets and dried to constant mass before testing. The initial dry mass of each specimen was measured using an analytical balance with an accuracy of ±0.1 mg. The specimens were then immersed in kerosene at room temperature. At predetermined time intervals, the samples were removed, lightly blotted with filter paper to remove excess surface liquid, and weighed immediately. The procedure was continued until no significant mass change was observed, indicating that equilibrium uptake had been reached.

The solvent-uptake behavior was used to compare the absorption characteristics among the different formulations. For comparative presentation of uptake behavior, the mass-uptake curves were plotted as M_t/M_0 against $t^{1/2}$, where M_0 is the initial dry mass of the specimen. For the initial stage of uptake, an apparent diffusion coefficient was estimated from the slope of the linear portion of the uptake curve using the conventional Fickian approximation for thin-sheet sorption [18, 19].

The equilibrium swelling index was calculated from the gravimetric mass increase according to:

where is the dry mass of the specimen and is the swollen mass at equilibrium.

For comparative interpretation, an apparent crosslink-related parameter was estimated from the equilibrium swelling data using a simplified Flory–Rehner-type treatment. The molar volume of the immersion liquid was estimated as V_s = 188.1 cm^3/mol, based on the average molecular weight and density of industrial-grade kerosene. Because kerosene is a multicomponent hydrocarbon mixture, the resulting swelling-based network parameter was used only for relative comparison among the studied formulations, rather than as an absolute thermodynamic crosslink-density value.

In this work, the swelling results are discussed as comparative indicators of solvent accessibility, transport restriction, and swelling resistance in the NR/NSS composites.

III. Results And Discussion

Characteristics of the Filler Materials

Fig. 1 shows a TEM micrograph of the nano-scale sewage sludge (NSS) filler. The image confirms the reduction of the primary particles to the nanoscale range (approximately 20-50 nm) and reveals a polycrystalline aggregate with non-uniform, irregular geometry. The sample exhibits a highly rugose surface, localized dark domains associated with diffraction contrast from more crystalline primary grains, and lighter regions that suggest a hierarchical porous architecture with appreciable inter-particle voids. Smaller semi-spherical protrusions and satellite particles around the periphery indicate agglomerative growth of primary nanoparticles into larger secondary structures. In addition, the presence of ultra-fine particles in the surrounding field suggests a broad particle-size distribution consistent with the processed sludge-derived filler.

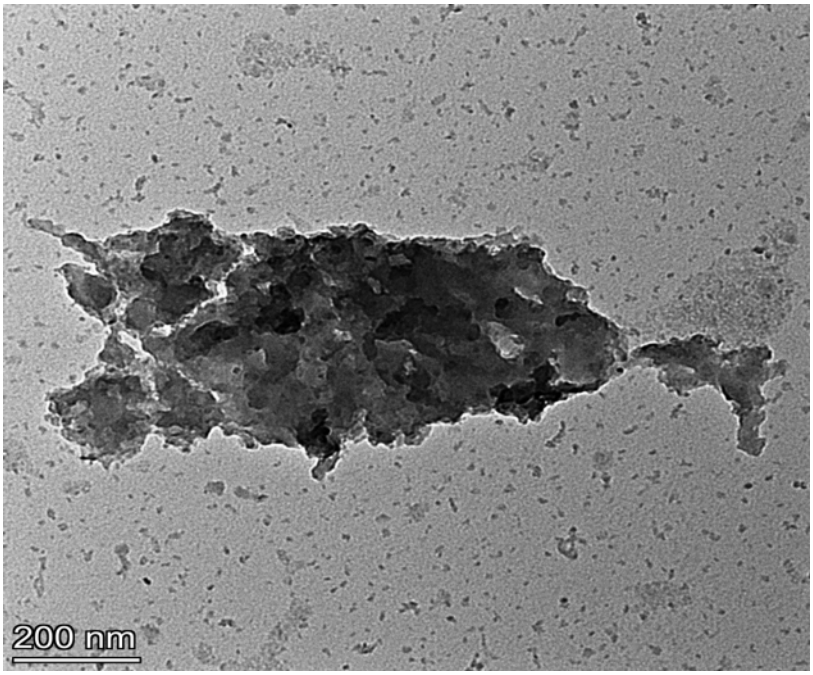

Fig. 1 TEM micrograph of Nano sewage sludge (NSS)

Fig. 2 complements the TEM observations by confirming the porous character of NSS through nitrogen adsorption/desorption analysis. BJH and DFT analyses indicated a mesoporous structure, with a BJH pore radius of about 1.78 -1.86 nm, a DFT cumulative surface area of 31.66 m^2/g, and a total pore volume of about 0.095 cm^3/g [15–17]. Because the multipoint BET fit showed poor linearity and an unphysical C constant, the textural discussion is based primarily on the BJH and DFT outputs.

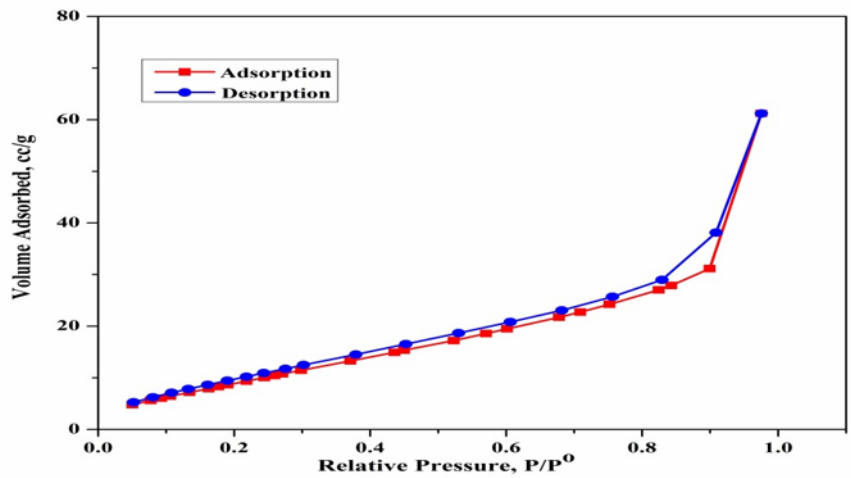

Fig. 2 Nitrogen adsorption-desorption isotherm of the nano-scale sewage sludge filler (NSS) at 77 K

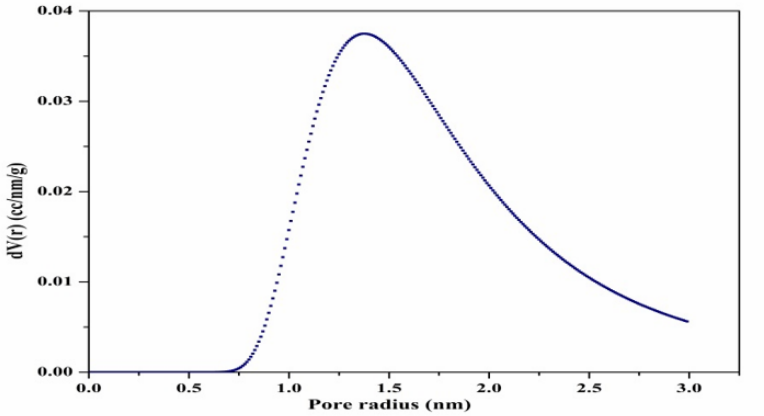

Fig. 3 Pore size distribution of the NSS filler calculated using the BJH method from the adsorption branch. The distribution is characterized by a dominant peak centered at a pore radius of approximately 1.78 nm, indicating a primary mesoporous channel

Fig. 4 shows SEM micrographs of NSS, revealing a heterogeneous and polydisperse architecture with irregular aggregates and a rough surface texture. Such morphological roughness can increase mechanical interlocking with the elastomer matrix. EDX analysis (Fig. 5) confirms a carbon-rich composition together with mineral constituents (e.g., O, Si, Al, Fe, and Ca), which can contribute to stiffness and thermal residue formation when incorporated into NR [13, 14].

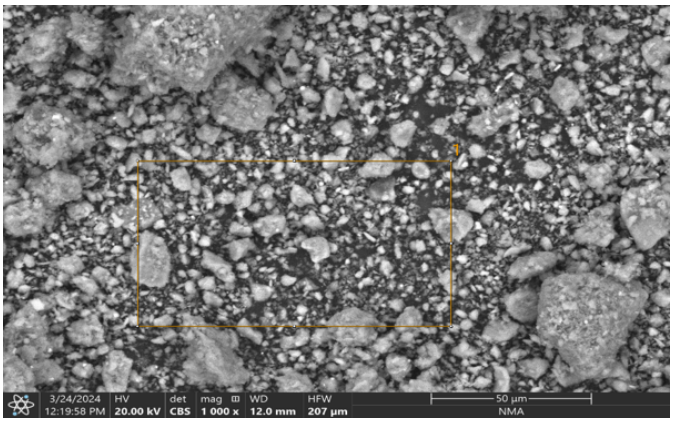

Fig. 4 Scanning Electron Microscopy (SEM) micrographs of the nano-scale sewage sludge filler (NSS)

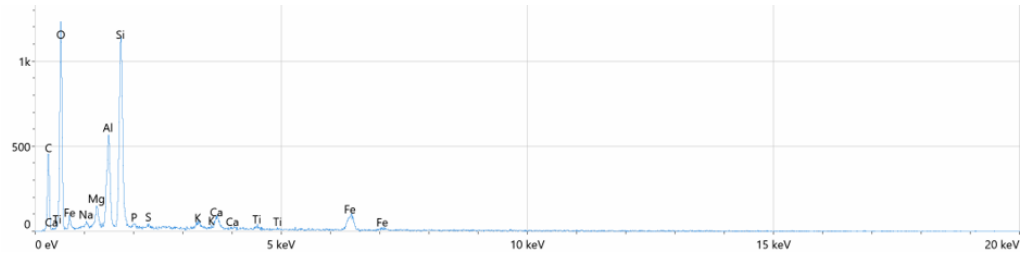

Fig. 5 Energy Dispersive X-ray Spectroscopy (EDX) spectrum and corresponding elemental composition of the NSS filler

Morphology Analysis

Analysis of the fracture surfaces provides critical insight into the load transfer mechanisms active across the filler–matrix interface, shown in Fig. 6. In the reference micrograph of neat NR, the fracture surface appears relatively smooth and almost featureless at this scale, with only gentle undulations and shallow tearing lines. The crack has propagated in a largely planar fashion through a continuous rubber matrix; the absence of rigid inclusions means that the crack is not forced to change direction or branch. Such a surface is typical of a ductile vulcanized elastomer where energy is dissipated mainly through large-scale chain extension and limited micro-cavitation within the bulk rather than through interactions with a second phase. This morphology

establishes the baseline: a homogeneous, highly deformable network with no external reinforcement influence [20–22].

Once 10 phr NSS is incorporated, the topography begins to deviate from that of the neat rubber. The surface becomes mildly granular, and a fine speckled contrast suggests the presence of well-dispersed nano-scale sludge domains that remain largely embedded in the matrix. The fracture plane is no longer perfectly flat; the crack path is gently deflected around these inclusions, creating a slightly roughened texture but still preserving an overall ductile character. Such a morphology signifies that filler–matrix adhesion is sufficient to avoid widespread debonding, yet the number of particles is not high enough to enforce a strongly tortuous crack route. This intermediate state is consistent with a modest increase in stiffness and tensile strength relative to pure NR, while the material still retains appreciable elongation at break.

At 30 phr NSS, the fracture surface becomes markedly more complex and highly energetic. The entire field is covered by a fine, densely packed relief; the crack path meanders in a convoluted fashion, repeatedly being forced to navigate around and between numerous well-dispersed filler domains. Many bright spots and faint pits indicate partial particle pull-out and local cavitation, yet the surrounding rubber appears tightly wrapped around these features, implying strong interfacial bonding. This combination of extensive crack deflection, local plastic deformation, and restricted particle debonding is consistent with efficient stress transfer from the NR matrix into the rigid nano-filler network, in line with classical descriptions of filler-mediated reinforcement in elastomers [20–22]. The morphology therefore substantiates the mechanical results, with 30 phr showing the most balanced fracture morphology: fracture requires higher energy because the advancing crack must continually detach rubber from the filler surface and thread through a highly constrained microstructure.

A very different picture emerges at the highest loading of 50 phr NSS. The surface is dominated by large, irregular agglomerates of sludge filler surrounded by dark gaps and distinct interfacial voids. These voids are not small pull-out cavities but extended regions where the matrix has completely separated from the filler, leaving open gaps and occasionally microcracks radiating from the agglomerates. Such features act as pre-existing flaws with severe local stress concentration; once the composite is loaded in tension, crack initiation occurs readily at these weak interfaces, and propagation can proceed along the agglomerate–matrix boundaries with comparatively little resistance. The fracture surface between agglomerate clusters appears comparatively flat, confirming that the crack finds an energetically easy route through the poorly bonded particle network rather than being repeatedly pinned and deflected as in the 30 % sample. This poor adhesion directly accounts for the rapid drop in tensile strength and the pronounced loss of elongation at high NSS contents; the rubber network is locally fragmented by rigid clusters that no longer cooperate with the matrix in carrying load, behavior consistent with agglomeration-driven failure in other waste-derived NR composites.

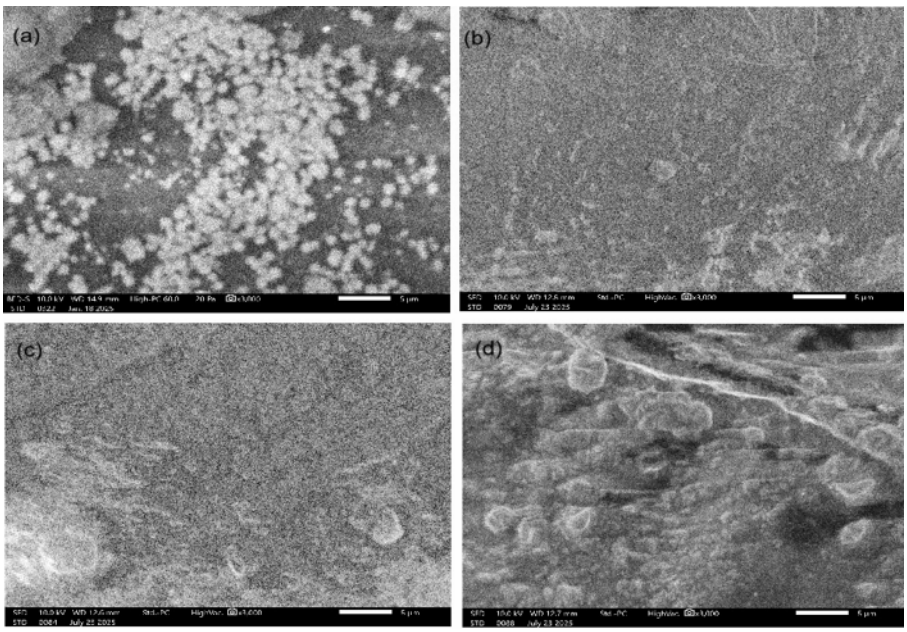

Fig. 6 Comparative Scanning Electron Microscopy (SEM) micrographs for Natural Rubber (NR) composites at various NSS filler loadings: (a) Pure NR (0 phr); (b) 10 phr loading; (c) 30 phr loading; and (d) 50 phr loading

Thermal Analysis

Thermal Stability and Decomposition Kinetics

Fig. 7 presents the thermal decomposition behavior of the NR/NSS composites at selected filler loadings. The TGA curves in Fig. 7(a), plotted as weight (%) versus temperature, show that all formulations remain relatively stable at lower temperatures before undergoing their main decomposition step within the temperature range associated with degradation of the rubber matrix and other organic constituents. As the NSS loading increases, the residual weight at high temperature increases markedly. This trend is expected because the sludge-derived filler contains inorganic and mineral constituents that are less thermally decomposable than the organic rubber phase. A broadly similar increase in residual fraction and change in decomposition profile has also been reported for recycled glass-filled NR composites, where the inorganic filler contribution increased the remaining mass after heating [7]. Accordingly, the higher final residue of the filled composites should be interpreted primarily as a compositional effect arising from the inorganic fraction of NSS rather than as direct proof of strong intrinsic thermal stabilization of the polymer matrix itself.

The DTG curves in Fig. 7(b) show that the main degradation-rate peak remains concentrated in the same general temperature region, while the peak height decreases progressively with increasing NSS content. This reduction in peak intensity is consistent with the dilution of the degradable rubber fraction and with the increasing contribution of non-volatile inorganic residue. Therefore, the DTG results are interpreted here as comparative changes in decomposition profile and rate behavior, rather than as conclusive evidence of major kinetic stabilization in the absence of additional numerical kinetic analysis.

Taken together, the TGA/DTG results indicate that increasing NSS loading modifies the thermal decomposition behavior of the composites and increases the residual fraction after heating. Within the scope of the present data, the most evident thermal effect of NSS is the increase in final residue and the change in degradation profile caused by the inorganic/carbonaceous filler fraction.

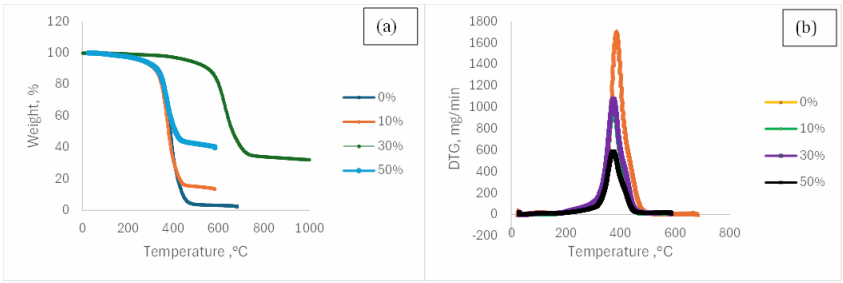

Fig. 7 Comparative thermal behavior of NR/NSS composites at selected NSS loadings: (a) TGA weight (%) curves and (b) DTG curves as a function of temperature.

Glass Transition and Thermal Transitions (DSC)

Fig. 8 shows the DSC thermograms of the NR/NSS composites at selected filler loadings. The DSC curves reveal differences in heat-flow response among the formulations over the scanned temperature range, reflecting differences in composition and thermal events associated with the rubber matrix and the sludge-derived filler.

In the revised interpretation, the DSC traces are used comparatively to show that NSS loading changes the overall thermal response of the composite system. As the filler content increases, the magnitude and profile of the heat-flow signal change, which may be attributed to the increasing contribution of the inorganic/carbonaceous filler fraction and to changes in the relative amount of thermally active organic material. In this sense, the filled composites exhibit a more attenuated heat-flow response than the unfilled rubber.

For clarity, the 0 phr sample corresponds to unfilled NR, not to pure sludge. The DSC discussion has therefore been revised accordingly. The present DSC results are interpreted as comparative thermal-response data that reflect formulation-dependent differences in composition and heat-flow behavior, rather than as evidence for a specific discrete transition assigned solely to the sludge filler without additional supporting analysis.

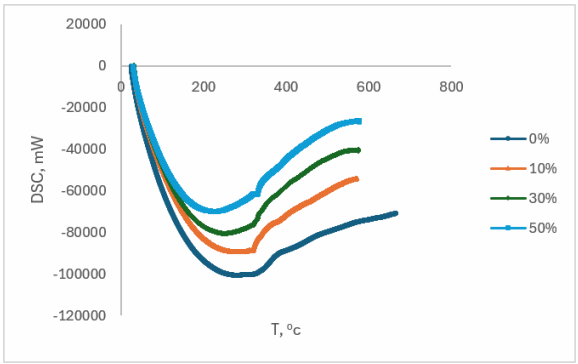

Fig. 8 Comparative Differential Scanning Calorimetry (DSC) thermograms of the Natural Rubber (NR) composites for 0, 10, 30, and 50 phr additive

Swelling Measurement and Crosslink Density

The kerosene-uptake behavior of the NR/NSS composites provides comparative insight into the effect of filler loading on solvent accessibility and transport through the rubber matrix. As shown in Fig. 9, the relative mass uptake changes systematically with increasing NSS content. The unfilled compound exhibits the highest solvent uptake over the immersion period, whereas the filled systems show progressively lower uptake as the filler loading increases. This trend indicates that the incorporation of NSS restricts solvent penetration into the NR matrix.

The decrease in solvent uptake with increasing NSS loading may be attributed to two related effects. First, the sludge-derived filler occupies part of the available free volume within the rubber compound, thereby reducing the fraction of the matrix accessible to the solvent. Second, the dispersed filler particles increase the tortuosity of the transport pathway, forcing kerosene molecules to follow a more complex route through the composite. As a result, the filled vulcanizates show lower swelling tendency than the unfilled rubber.

A similar trend is observed for the apparent diffusion behavior shown in Fig. 10. The apparent diffusion coefficient decreases as the NSS loading increases, indicating that solvent transport becomes progressively slower in the presence of the filler. This behavior is consistent with reduced penetrant mobility in the composite structure and with the formation of a more obstructed pathway for solvent ingress.

The equilibrium swelling index in Fig. 11 decreases progressively with increasing NSS loading, indicating that the filled composites absorb less kerosene at equilibrium than the unfilled rubber. This trend reflects reduced solvent accessibility in the NR matrix and may be associated with partial free-volume occupation by the filler, increased transport-path tortuosity, and restricted chain mobility near the filler domains.

For comparative purposes, Fig. 11 also presents an apparent crosslink-related parameter estimated from the equilibrium swelling data. The increase of this parameter with NSS loading is consistent with the observed reduction in swelling tendency. Since industrial-grade kerosene is a multicomponent hydrocarbon mixture, this parameter is used only for relative comparison among the studied formulations, rather than as an absolute thermodynamic crosslink-density value. Taken together, these results indicate that increasing NSS content improves swelling resistance and hinders solvent transport in the NR matrix.

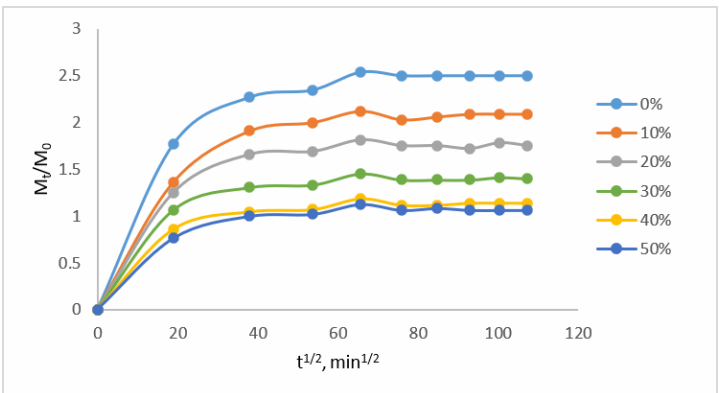

Fig. 9 Relative mass uptake (M_t/M_0) as a function of square-root time for NR/NSS composites at selected NSS loadings

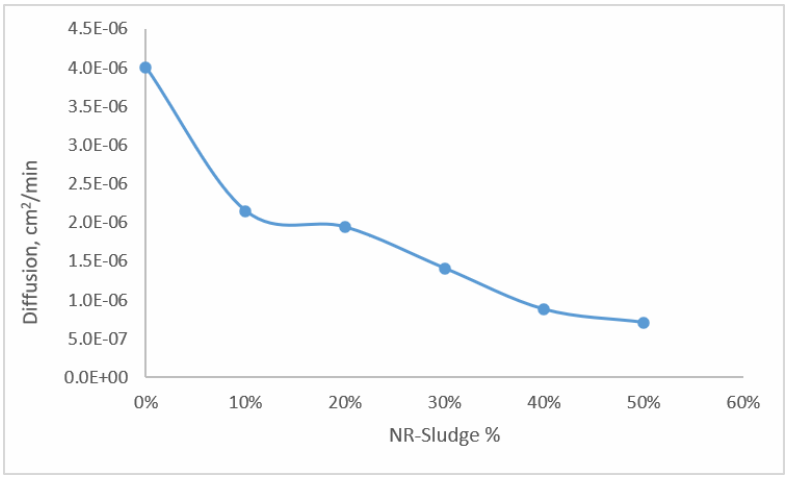

Fig. 10 Apparent diffusion coefficient of kerosene in NR/NSS composites as a function of NSS loading

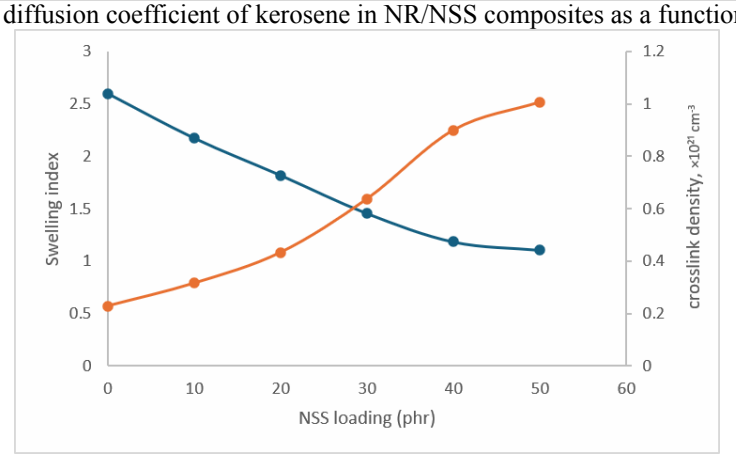

Fig. 11 Variation of equilibrium swelling index and apparent crosslink-related parameter with NSS loading

Shore A Hardness

The Shore A hardness of the NR/NSS composites increases progressively with increasing NSS loading, as shown in Fig. 12. In comparison with the unfilled rubber, the filled composites exhibit a clear increase in resistance to indentation, indicating that the sludge-derived filler acts as a rigid dispersed phase within the softer NR matrix. This trend is consistent with reduced local deformability and with restriction of chain mobility in the presence of filler particles.

The monotonic increase in hardness with filler loading can be attributed mainly to the increasing volume fraction of the relatively rigid NSS phase and to the corresponding reduction in the compliance of the rubber compound. As more filler is incorporated, the composite becomes less susceptible to localized deformation under the indenter, resulting in higher Shore A values. From a practical standpoint, this behavior indicates that NSS is effective in increasing compound stiffness at the surface scale, even though the overall mechanical performance must still be evaluated together with tensile properties and morphology.

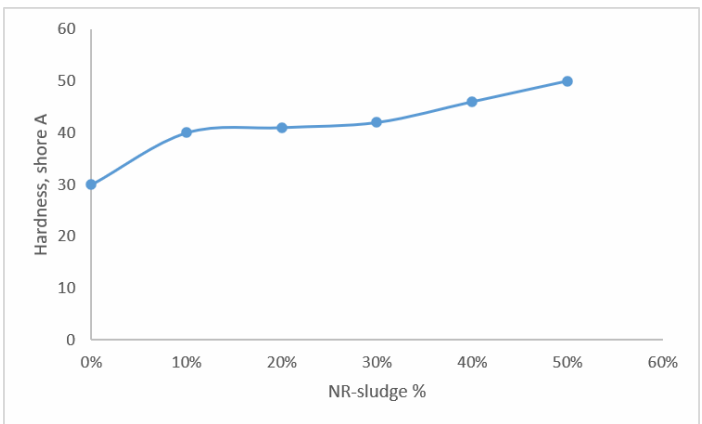

Fig. 12 Variation of hardness with Sewage sludge content

Tensile Response and Stiffness Evolution

The tensile behavior of the NR/NSS composites is shown in Figs. 13 and 14. The inclusion of the 0 phr formulation in the revised dataset allows direct comparison between the unfilled rubber and the filled compounds. Relative to unfilled NR, the incorporation of NSS leads to a pronounced increase in modulus and an overall improvement in tensile response, confirming that the sludge-derived filler does not act merely as an inert diluent within the studied composition range [20–22].

The stress-strain curves show that the addition of NSS changes the mechanical response of the composites from that of a softer and more compliant rubber to that of a progressively stiffer material. This is reflected in the increase in modulus with filler loading, indicating that the dispersed filler phase increasingly restricts elastic deformation of the NR matrix under tensile load. Comparable stiffness enhancement with increasing filler loading, followed by deterioration in overall reinforcement efficiency at excessive loading due to aggregation effects, has also been observed in recycled glass-filled rubber systems [7, 8]. In this sense, NSS contributes to stress transfer and increases resistance to deformation, particularly at higher loadings [20–22].

At the same time, the tensile results should be interpreted together with the morphological observations. While the higher loadings provide greater stiffness and higher stress levels, the fracture-surface analysis indicates that excessive filler content is also associated with greater agglomeration and less favorable interfacial uniformity. Accordingly, the mechanical data suggest that NSS loading enhances stiffness and can improve tensile performance relative to unfilled NR, whereas the morphology indicates that increasing filler content also introduces structural heterogeneity that may limit reinforcement efficiency at high loading.

Therefore, the effect of NSS cannot be described by a single optimum criterion for all properties. From the mechanical point of view, the higher-loading formulations exhibit the greatest stiffness and the highest stress levels. However, from the microstructural point of view, intermediate loading shows a more balanced morphology with less pronounced agglomeration. The overall results thus indicate that NSS can improve the tensile rigidity of NR composites, while the final balance between stiffness, strength, and structural uniformity remains strongly dependent on filler loading and dispersion quality.

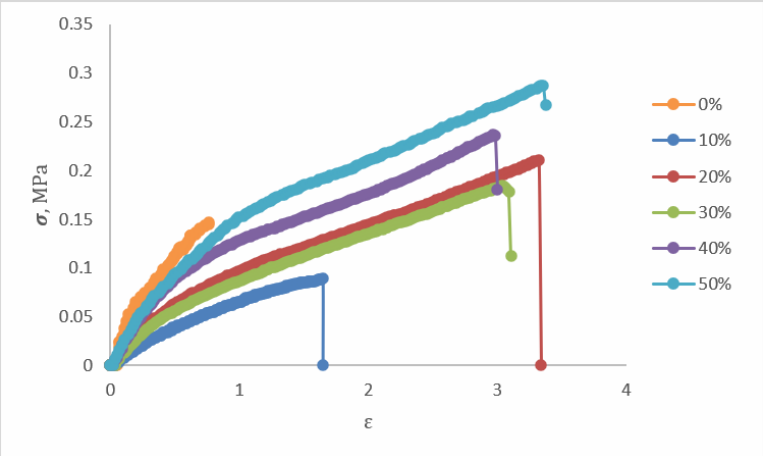

Fig. 13 Comparative Stress-Strain curves of Natural Rubber (NR) composites as a function of NSS filler loading

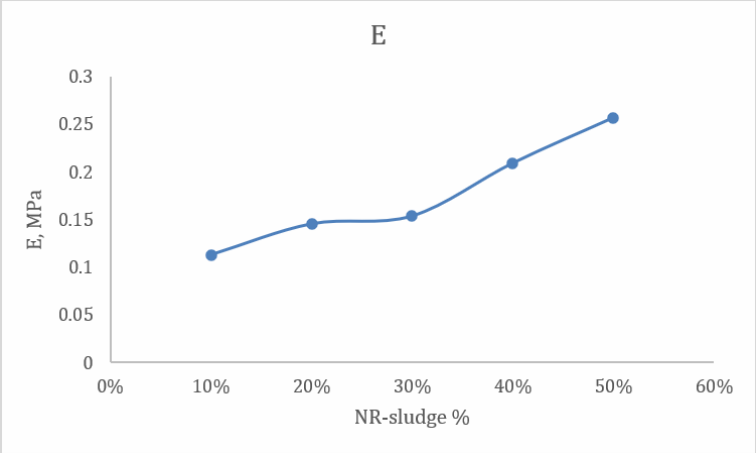

Fig. 14 Variation of tensile modulus of NR/NSS composites with NSS loading

IV. Conclusion

This study demonstrates that dewatered municipal sewage sludge can be processed into a functional waste-derived filler for natural rubber composites through drying, grinding, and high-energy milling. The resulting NSS filler altered the morphology, mechanical behavior, swelling response, and thermal decomposition profile of the NR matrix, confirming that sewage-sludge-derived solids can serve as more than a simple inert extender in rubber compounding.

The experimental results show that increasing NSS loading progressively increases hardness and tensile modulus and reduces kerosene uptake and apparent diffusion behavior, indicating greater resistance to deformation and lower solvent accessibility in the filled composites. Thermal analysis further showed that NSS increases the residual fraction after heating, mainly because of its inorganic/mineral content, while also modifying the overall decomposition profile of the composites. At the same time, the results also indicate that higher filler loading is accompanied by greater structural heterogeneity and agglomeration, as observed in the fracture morphology.

Accordingly, the role of NSS should be interpreted in a balanced way. From the mechanical point of view, higher filler loading enhances stiffness and improves tensile response relative to unfilled NR within the studied formulations. From the microstructural point of view, however, intermediate loading provides a more favorable balance between dispersion quality and property development, whereas excessive loading promotes agglomeration and less uniform fracture features. Therefore, the final performance of NR/NSS composites depends strongly on filler loading, dispersion state, and the targeted application criterion.

From an application standpoint, the present results suggest that NSS-filled NR is more promising for semi-structural and general-purpose rubber products where stiffness, hardness, and reduced swelling are desirable, rather than for applications requiring highly optimized reinforcement efficiency comparable to conventional high-performance carbon black or silica systems. The study therefore supports NSS as a low-cost waste-derived filler with potential value in selected rubber products, while also highlighting the need for further work on cure optimization, filler standardization, hybrid filler design, durability testing, and techno-economic assessment before large-scale industrial implementation.

Statements and Declarations

Funding

No funding was received to assist with the preparation of this manuscript

Competing interests

The author declare that they have no competing interests.

Data availability

Available on reasonable request.

Ethics approval

Not applicable.

Clinical trial number: not applicable.

Consent to participate

Not applicable

Consent for publication
Not applicable

References

[1]. Fytili D, Zabaniotou A (2008) Utilization Of Sewage Sludge In EU Application Of Old And New Methods-A Review. Renew Sustain Energy Rev 12(1):116-140. Https://Doi.Org/10.1016/J.Rser.2006.05.014
[2]. Kelessidis AS, Stasinakis AS (2012) Comparative Study Of The Methods Used For Treatment And Final Disposal Of Sewage Sludge In European Countries. Waste Manag 32(6):1186-1195. Https://Doi.Org/10.1016/J.Wasman.2012.01.012
[3]. Abdel Wahaab R, Mahmoud M, Van Lier JB (2020) Toward Achieving Sustainable Management Of Municipal Wastewater Sludge In Egypt: Challenges And Opportunities. Renew Sustain Energy Rev 127:109880. Https://Doi.Org/10.1016/J.Rser.2020.109880
[4]. Fini EH, Kazemi M, Poulikakos L, Lazorenko G, Akbarzade V, Lamanna A, Lammers P (2024) Perspectives On Innovative Non-Fertilizer Applications Of Sewage Sludge For Mitigating Environmental And Health Hazards. Commun Eng 3:178. Https://Doi.Org/10.1038/S44172-024-00298-X
[5]. Chang BP, Akil HM, Nasir RM, Abdul Razak SI, Zulkepli NN (2021) Toward Bioresourced Fillers For Rubber Composites: A Review. Green Chem 23:7628-7654. Https://Doi.Org/10.1039/D1GC01115D
[6]. Dadkhah M, Messori M (2024) A Comprehensive Overview Of Conventional And Bio-Based Fillers For Rubber Formulations Sustainability. Mater Today Sustain 27:100886. Https://Doi.Org/10.1016/J.Mtsust.2024.100886
[7]. Moubarak DI, Elrasasi TY (2025) Influence Of Micro-Glass Fillers On The Mechanical And Thermal Properties Of Natural Rubber Composites. Egypt J Solids 74:167-199.
[8]. Moubarak DI, Hanafy M, Elrasasi TY, Elbashar YH (2024) Impact Of Recycled Micro-Gray Glass Grains On The Mechanical Properties Of SBR And NBR. Physics AUC 34:221-228.
[9]. Intiya W, Thepsuwan U, Sirisinha C, Sae-Oui P (2017) Utilization Of Incinerated Sewage Sludge Ash As A Filler In Natural Rubber Composites. J Mater Cycles Waste Manag 19:774-781. Https://Doi.Org/10.1007/S10163-016-0480-5
[10]. Fan Y, Fowler GD, Norris C (2025) The Development Of Pyrolytic Sewage Sludge Char As A Novel Bio-Filler For Styrene-Butadiene Rubber. Waste Biomass Valor. Https://Doi.Org/10.1007/S12649-025-03157-8
[11]. Schouw C, Bernal-Ortega P, Anyszka R, Bijl A, Gucho E, Blume A (2025) Toward Eco-Friendly Rubber: Utilizing Paper Waste-Derived Calcium Carbonate To Replace Carbon Black In Natural Rubber Composites. J Compos Sci 9(3):115. Https://Doi.Org/10.3390/Jcs9030115
[12]. Inphonlek S, Bureewong N, Kotchapradit S, Ruksakulpiwat Y, Ruksakulpiwat C (2025) Synergistic Effects Of Hybrid Bio-Fillers And Modified Natural Rubber On Natural Rubber Composite Properties. Polymers 17(5):632. Https://Doi.Org/10.3390/Polym17050632
[13]. Goldstein J, Newbury DE, Ritchie NWM, Michael JR, Scott JHJ, Joy DC (2018) Scanning Electron Microscopy And X-Ray Microanalysis, 4th Edn. Springer, New York. Https://Doi.Org/10.1007/978-1-4939-6676-9
[14]. Williams DB, Carter CB (2009) Transmission Electron Microscopy: A Textbook For Materials Science, 2nd Edn. Springer, New York. Https://Doi.Org/10.1007/978-0-387-76501-3
[15]. Thommes M, Kaneko K, Neimark AV, Olivier JP, Rodriguez-Reinoso F, Rouquerol J, Sing KSW (2015) Physisorption Of Gases, With Special Reference To The Evaluation Of Surface Area And Pore Size Distribution (IUPAC Technical Report). Pure Appl Chem 87(9-10):1051-1069. Https://Doi.Org/10.1515/Pac-2014-1117
[16]. Brunauer S, Emmett PH, Teller E (1938) Adsorption Of Gases In Multimolecular Layers. J Am Chem Soc 60(2):309-319. Https://Doi.Org/10.1021/Ja01269a023
[17]. Barrett EP, Joyner LG, Halenda PP (1951) The Determination Of Pore Volume And Area Distributions In Porous Substances. I. Computations From Nitrogen Isotherms. J Am Chem Soc 73(1):373-380. Https://Doi.Org/10.1021/Ja01145a126
[18]. Crank J (1975) The Mathematics Of Diffusion, 2nd Edn. Clarendon Press, Oxford
[19]. Ritger PL, Peppas NA (1987) A Simple Equation For Description Of Solute Release II. Fickian And Anomalous Release From Swellable Devices. J Control Release 5(1):37-42. Https://Doi.Org/10.1016/0168-3659(87)90035-6
[20]. Pukánszky B (1990) Influence Of Interface Interaction On The Ultimate Tensile Properties Of Polymer Composites. Composites 21(3):255-262. Https://Doi.Org/10.1016/0010-4361(90)90240-W
[21]. Heinrich G, Klüppel M (2002) Rubber Reinforcement By Filler Networking: Theory And Application. Adv Polym Sci 160:1-44. Https://Doi.Org/10.1007/3-540-45362-8_1
[22]. Litvinov VM, Orza RA, Klüppel M, Van Duin M, Magusin PCM (2011) Rubber-Filler Interactions And Network Structure In Relation To Stress-Strain Behavior Of Filled Vulcanizates. Macromolecules 44(12):4887-4900. Https://Doi.Org/10.1021/Ma2007255